Sādhanā Vol. 28, Part 6, December 2003, pp. 1027–1035.

Time-variant power spectral analysis of heart-rate time series by autoregressive moving average (ARMA) method

V P S NAIDU and M R S REDDY

Biomedical Engineering Division, Indian Institute of Technology - Madras, Chennai 600 035, India
e-mail: vpsnaidu_nal@yahoo.co.in

MS received 13 December 2002; revised 9 September 2003

Abstract. Frequency domain representation of a short-term heart-rate time series (HRTS) signal is a popular method for evaluating the cardiovascular control system. The spectral parameters, viz. percentage power in low frequency band (%PLF), percentage power in high frequency band (%PHF), power ratio of low frequency to high frequency (PRLH), peak power ratio of low frequency to high frequency (PPRLH) and total power (TP) are extrapolated from the averaged power spectrum of twenty-five healthy subjects, and 16 acute anterior-wall and nine acute inferior-wall myocardial infarction (MI) patients. It is observed that parasympathetic activity predominates in healthy subjects. From this observation we conclude that during acute myocardial infarction, the anterior wall MI has stimulated sympathetic activity, while the acute inferior wall MI has stimulated parasympathetic activity. Results obtained from ARMA-based analysis of heart-rate time series signals are capable of complementing the clinical examination results.

Keywords. Heart-rate variability; medical signal processing; auto regressive moving average model.

1. Introduction

The normal rhythm of a heart is prone to sudden stress and impulses acting on the cardiovascular system. This non-stationarity in the rhythm is reflected on cardiovascular variables such as heart-rate and blood pressure, even when environmental parameters are maintained at a constant level. Variation of sinus rate over a time interval is termed the heart-rate time series (HRTS) or heart-rate variability (HRV). The two branches of the autonomic nervous system (ANS), called sympathetic and parasympathetic control systems, influence cardiovascular functions. The non-stationary nature of ANS causes the spectral contents of HRT series to vary with time in two frequency bands, which are named sympathetic (0·05 to 0·15 Hz) and parasympathetic (0·18 to 0·4 Hz) bands (Naidu *et al* 1999). The HRT series is related to various cardiovascular disorders, which lead to oscillations about the mean heart-rate.

The power spectral analysis of HRT series is a non-invasive method to assess the autonomic nervous system control of the heart, both in normal and abnormal subjects. The advantage of power spectral analysis of the HRT series is the possibility of studying frequency-specific oscillations. Power spectral analysis involves decomposition of a series of sequential R-point to R-point intervals into a sum of sinusoidal functions of different amplitudes and frequencies. The result could be displayed with varying magnitude as a function of frequency, which is called power spectrum of HRT series. It reflects the amplitude of the heart-rate fluctuations present at different frequencies. Fast Fourier Transformation (FFT) analysis is used generally to transform signals into the frequency domain. This method has a few technical limitations such as, (a) use of deterministic algorithms that are valid only to periodic phenomena, (b) Necessity of windowing the data, and (c) uncertainty in defining the relative powers of the various spectral components (Pagani *et al* 1976; Natalucci *et al* 1999).

The Autoregressive Moving Average (ARMA)-based method eliminates these limitations, as they do not require windowing or filtering of the data (Marple 1987). This paper reports preliminary data collection from twenty-five normal and twenty-five myocardial infarction (MI) patients. ARMA-based comparative analysis of the HRT series power spectrum of both sets of people has been carried out.

2. Materials and methods

Five hundred and twelve (512) samples of HRT series were considered, which are quite reasonable for computing the power spectrum with good frequency resolution. About 448 epochs of 64 samples, overlapped by one sample (0·5 s), are extracted from the above series. With an ARMA-based method, HRT series power spectral density was estimated, epoch-by-epoch. The nth HRT series value was termed the output $y(n)$ of an ARMA model (as shown in figure 1) of order 'p', driven by an impulse sequence termed $x(n)$.

In figure 1 $x(n)$ is the impulse sequence, $y(n)$ is HRT series, **B(z)** is the transfer function of the moving average (MA) method and **A(z)** is the transfer function of the auto regressive (AR) method.

$$y(n) + \sum_{k=1}^{p} a_k y(n-k) = \sum_{k=0}^{p} b_k x(n-k), n = 0, 1, 2, \ldots , N-1, \tag{1}$$

where a_k represents the AR coefficients of the AR process at the kth stage, b_k represents the MA coefficients of the MA process at the kth stage, N is the length of the sequence and p represents the model order. We need to find the transfer function $H(z) = Y(z)/X(z)$, whose impulse response $h(k)$ approximates $x(k)$, such that the sum of squared error 'e' is minimum, i.e.

$$e = \sum_{k=0}^{p} [h(k) - x(k)]^2, \text{ is minimum.} \tag{2}$$

The coefficients a_k and b_k have to be estimated by minimising 'e' (Baselli *et al* 1987; Kay 1988). The least squares solution to this problem is by direct minimisation of the error as a function of a_k and b_k, which requires a set of simultaneous equations. Below is the representation of (1) as a set of simultaneous equations.

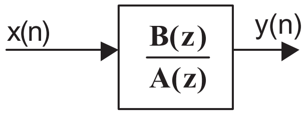

Figure 1. ARMA model representation.

$$
\begin{aligned}
y(0) &= -a_1 y(-1) - a_2 y(-2) - \ldots\ldots\ldots - a_p y(-p) + b_0 x(0) \\
&\quad + b_1 x(-1) + \ldots\ldots + b_p x(-p) \\
y(1) &= -a_1 y(0) - a_2 y(-1) - \ldots\ldots\ldots - a_p y(1-p) + b_0 x(1) \\
&\quad + b_1 x(0) + \ldots\ldots + b_p x(1-p) \\
&\qquad \ldots\ldots\ldots\ldots\ldots\ldots\ldots\ldots\ldots\ldots \\
&\qquad \ldots\ldots\ldots\ldots\ldots\ldots\ldots\ldots\ldots\ldots \\
y(N-1) &= -a_1 y(N-2) - a_2 y(N-3) - \ldots\ldots - a_p y(N-1-p) \\
&\quad + b_0 x(N-1) + b_1 x(N-2) + \ldots\ldots + b_p x(N-1-p). \qquad (3)
\end{aligned}
$$

Equation (3) can also be expressed in matrix notation as

$$\mathbf{Y} = \mathbf{AX}, \qquad (4)$$

where $\mathbf{Y}$ is the output matrix $(N, 1)$, $\mathbf{A}$ is input–output parameter matrix $(\mathbf{N}, 2p+1)$ and $\mathbf{X}$ is the ARMA parameter (coefficients a_k, b_k) matrix $(2p+1, 1)$. Its matrix representation is shown below.

$$
\begin{bmatrix} y(0) \\ y(1) \\ y(2) \\ \cdot \\ \cdot \\ \cdot \\ \cdot \\ y(N-2) \\ y(N-1) \end{bmatrix}
=
\begin{bmatrix}
y(-1) & y(-2) & \cdot\ \cdot & y(-p) & x(0) & x(-1) & \cdot\ \cdot & x(-p) \\
y(0) & y(-1) & \cdot\ \cdot & y(1-p) & x(1) & x(0) & \cdot\ \cdot & x(1-p) \\
y(1) & y(0) & \cdot\ \cdot & y(2-p) & x(2) & x(1) & \cdot\ \cdot & x(2-p) \\
\cdot & \cdot & \cdot\ \cdot & \cdot & \cdot & \cdot & \cdot\ \cdot & \cdot \\
\cdot & \cdot & \cdot\ \cdot & \cdot & \cdot & \cdot & \cdot\ \cdot & \cdot \\
\cdot & \cdot & \cdot\ \cdot & \cdot & \cdot & \cdot & \cdot\ \cdot & \cdot \\
\cdot & \cdot & \cdot\ \cdot & \cdot & \cdot & \cdot & \cdot\ \cdot & \cdot \\
y(N-3) & y(N-4) & \cdot\ \cdot & y(N-2-p) & x(N-2) & x(N-3) & \cdot\ \cdot & x(N-2-p) \\
y(N-2) & y(N-3) & \cdot\ \cdot & y(N-1-p) & x(N-1) & x(N-2) & \cdot\ \cdot & x(N-1-p)
\end{bmatrix}
\begin{bmatrix} -a_1 \\ -a_2 \\ \cdot \\ \cdot \\ -a_p \\ b_0 \\ b_1 \\ \cdot \\ \cdot \\ b_p \end{bmatrix}
$$

For solving the matrix $\mathbf{Y} = \mathbf{AX}$, there are a larger number of equations than of unknown parameters, which is called an over-determined system. In this case, let us define an error signal:

$$e = \mathbf{Y} - \mathbf{AX}. \qquad (5)$$

Minimizing the squared norm of e, i.e. find $\mathbf{X}$ to minimize $e^T e$, to obtain the solution. The matrix denoted e^T is transpose of the matrix e,

$$e^T e = (Y - AX)^T (Y - AX) = (Y^T Y - X^T A^T Y - Y^T AX + X^T A^T AX). \qquad (6)$$

The terms $X^T A^T Y$ and $Y^T AX$ are scalars with equal magnitudes. The vector indicated as $\mathbf{X}^T$ is the transpose of the vector X. To minimise the above equation (6), differentiate both the sides with respect to X^T and equate to zero.

$\frac{\partial}{\partial X^T}(e^T e) = (-A^T Y + A^T AX) = 0$, hence, it can be written as $A^T Y = A^T AX$, From the above equation, the unknown vector X (ARMA parameters) can be computed as

$$X = (A^T A)^{-1} A^T Y. \qquad (7)$$

The above equation is known as the least squares solution for an over-determined set of linear equations. The term $(A^T A)^{-1} A^T$ is named the pseudo inverse operator (Naidu *et al*).

The HRT series is assumed to be stationary within each epoch. The order of the model 'p' is chosen as ten, which is a reasonable average value to discriminate the main frequency components accurately (Pina *et al* 1992; Natalucci *et al* 1999). Power spectral density estimation, PSD (f) was obtained from the relation:

$$\mathrm{PSD}\ (f) = t \left| \sum_{k=0}^{p} b_k e^{-i2\Pi fkt} \right|^2 \Bigg/ \left| 1 + \sum_{k=0}^{p} a_k e^{-i2\Pi fkt} \right|^2, \tag{8}$$

where 't' is the inverse of the sampling frequency f_s (2 Hz) (Baselli *et al* 1987; Kay 1988). In the spectral analysis, the two ranges of frequencies of interest, 0·05–0·15 Hz (low frequency band) and 0·18–0·4 Hz (high frequency band), correspond to the sympathetic and parasympathetic activities respectively (Naidu *et al* 1999). The power concentrated in the LF (PLF) and HF (PHF) bands are estimated by integrating the above power spectrum. The peak power in the LF (PPLF) and HF (PPHF) bands and the total power (TP $=$ PLF $+$ PHF) are also estimated. Similarly, the percentage power distribution in LF (%PLF $=$ PLF $*$ 100/TP) and HF (%PHF $=$ PHF $*$ 100/TP) bands are computed.

3. Results and discussion

3.1 *Simulation*

The performance of the above technique was verified using simulated signals. A model was designed for generation of simulated HRT series signal as shown in figure 2. Two simulated signals were generated in such a way that sympathetic activity was greater $(A > B)$ in the first simulation signal $sp(n)$ and parasympathetic activity was greater $(A < B)$ in the second simulation signal '$psp(n)$', where A and B are amplitudes of sinusoidal signals. The simulated signals are shown in figure 3.

These simulated signals were obtained from the following functions.

$$sp(n) = 0{\cdot}8 + 0{\cdot}125 \sin(2\Pi f_l n/fs) + 0{\cdot}0625 \sin(2\Pi f_h n/fs) + w(n), \tag{9}$$

$$psp(n) = 0{\cdot}8 + 0{\cdot}0625 \sin(2\Pi f_l n/fs) + 0{\cdot}125 \sin(2\Pi f_h/fs) + w(n), \tag{10}$$

where, $w(n)$ is the white noise added to the sinusoids in order to obtain a broad-band signal, constant 0·8 is added since the usual duration of the cardiac cycle is around 800ms, f_l is stable LF component ($f_l = 0{\cdot}1$ Hz), f_h is stable HF component ($f_h = 0{\cdot}3$ Hz) and sampling frequency f_s was selected as 2 Hz ($f_s = 2$ Hz), since the maximum frequency of interest in HRT series is around 0·5 Hz. Power spectrums were computed for the above two simulated signals. The overlaid realisation spectrum of heart-rate time series signal is shown in figure 4.

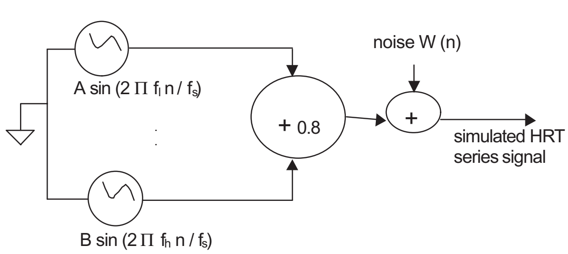

Figure 2. Design model for generation of simulated HRT series.

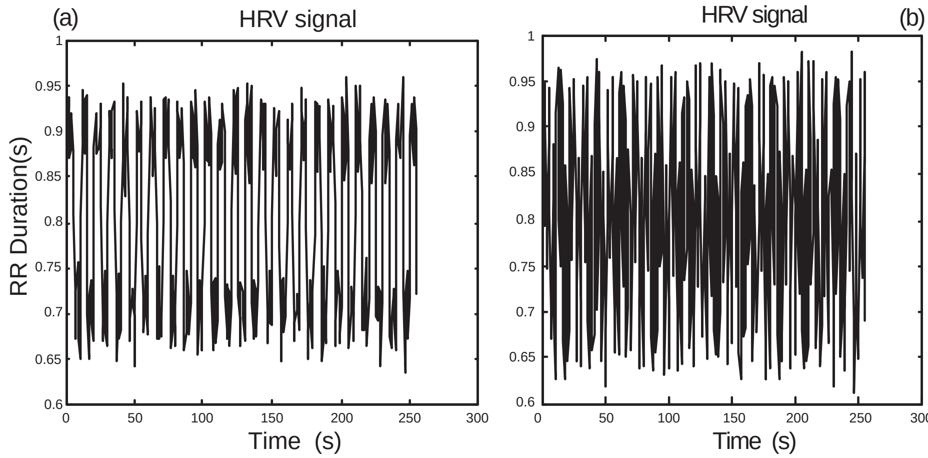

Figure 3. The simulated signals $sp(n)$ **(a)** and $psp(n)$ **(b)** respectively.

The three-dimensional view of heart-rate time series signal spectrum is shown in figure 5. The average of realisation of heart-rate time series signal spectrum is shown in figure 6. The parameters PLF, PPF, TP, PPLF and PPHF are extrapolated from the above spectrum. It is observed from the $sp(n)$ signal that PLF is greater than PHF and PPLF is greater than PPHF, and vice versa in the case of the $psp(n)$ signal.

3.2 *Experimental data collection*

Lead II surface ECG of twenty-five healthy subjects (15 males, 10 female) aged between 20 and 60 years, sixteen acute anterior wall MI patients (13 males, 3 female) aged between 50 and 70 years and nine acute inferior wall MI patients (7 males, 2 female) aged between 48 and 72 years for a duration of eight minutes were recorded at a sampling rate of 500 Hz with 12-bit resolution using an ADC card. Steps involved in the heart-rate time series analysis are indicated in figure 7. The output of the ECG acquisition system was given to an analog to digital conversion (ADC) card, to generate a digital data of 12-bit resolution and stored in the

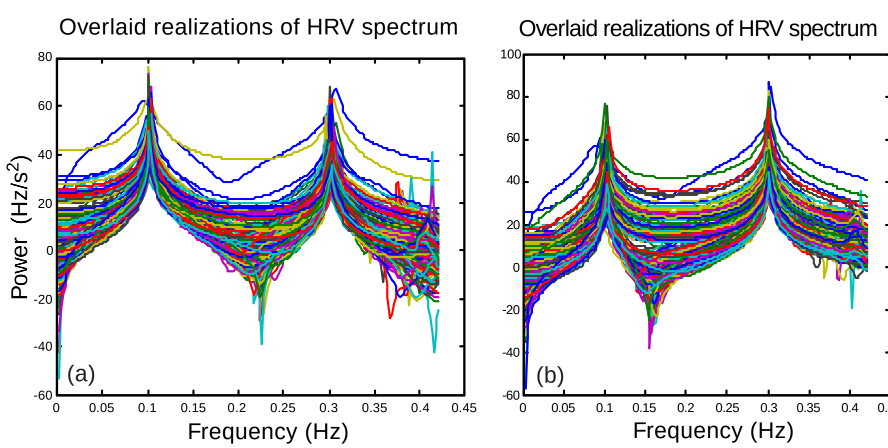

Figure 4. Overlaid realisation of $sp(n)$ **(a)** and $psp(n)$ **(b)** spectrum respectively.

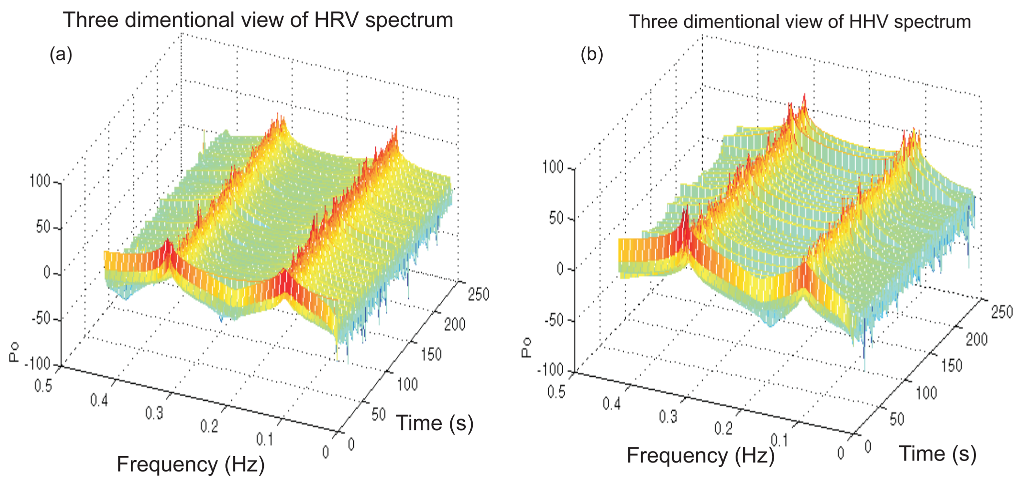

Figure 5. Three-dimensional view of $sp(n)$ **(a)** and $psp(n)$ **(b)** spectrums respectively.

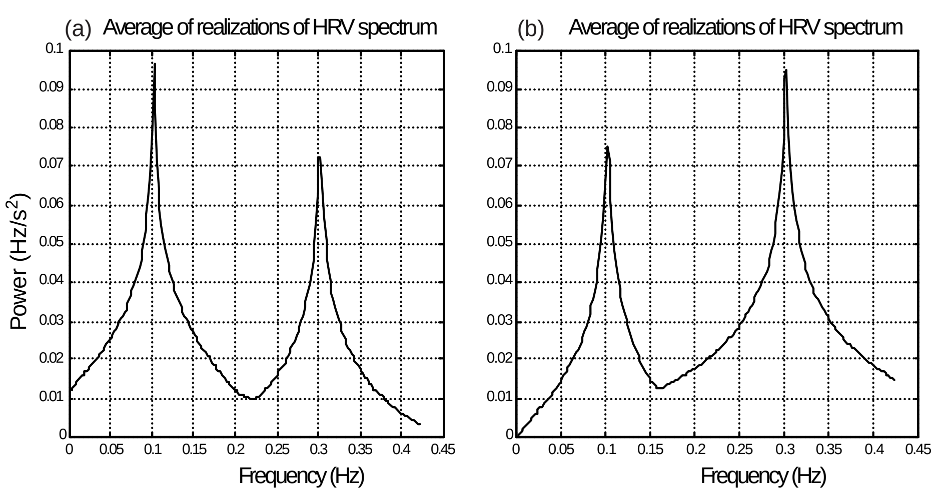

Figure 6. Average of realisation of $sp(n)$ **(a)** and $psp(n)$ **(b)** spectrum respectively.

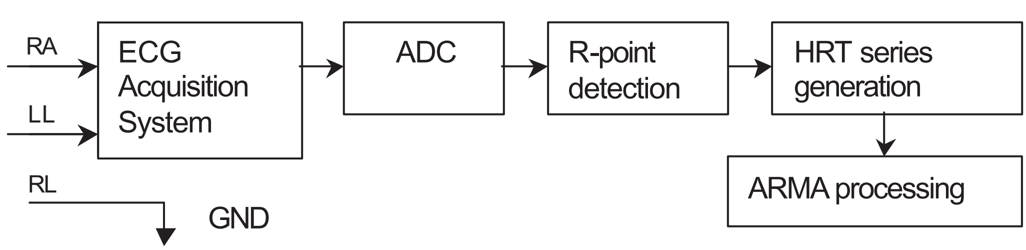

Figure 7. Steps involved in HRT series analysis.

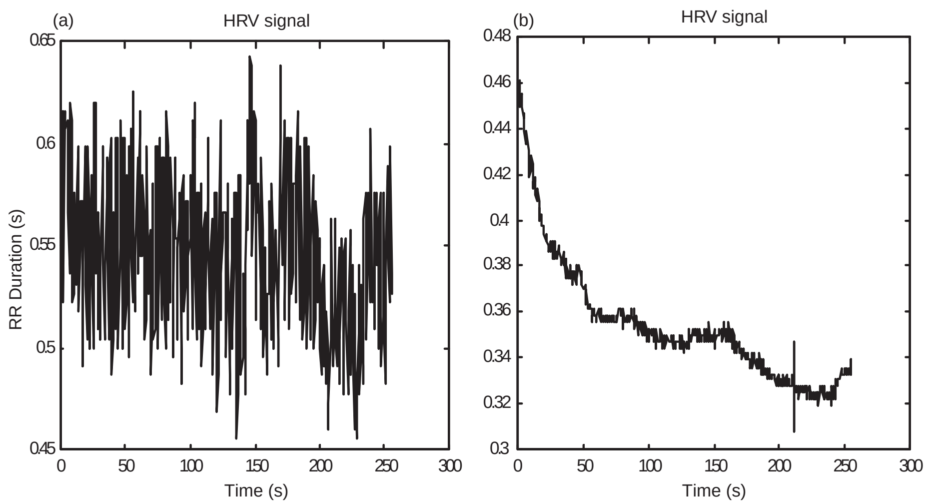

Figure 8. Heart-rate time series of control **(a)** and MI patient **(b)**.

PC memory simultaneously. R-points were detected from the acquired surface ECG (Naidu *et al* 2000). The HRT series was generated from the detected R-points (Naidu *et al* 1999) and subjected to ARMA processing.

The heart-rate time series signals of a normal person (control) and an MI patient are shown in figure 8 and overlaid realisation of heart-rate time series signal spectrum is shown in figure 9. Spikes are observed at LF and HF regions. A three-dimensional view of the heart-rate time series spectrum is shown in figure 10 and the average of realisation of heart-rate time series signal spectrum is shown in figure 11.

The parameters PRLH, PPRLH, TP, %PLF and %PHF are estimated from the above averaged spectrum. It is observed that more power is concentrated in the LF region in case of MI patient and vice versa in case of healthy subjects. The statistical results are showed in table 1.

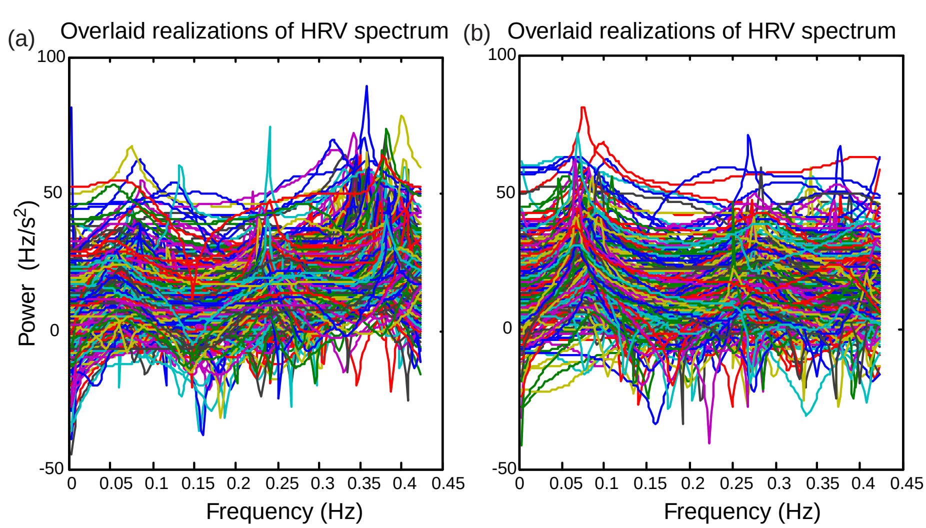

Figure 9. Overlaid realisation spectrum of control **(a)** and MI patient **(b)**.

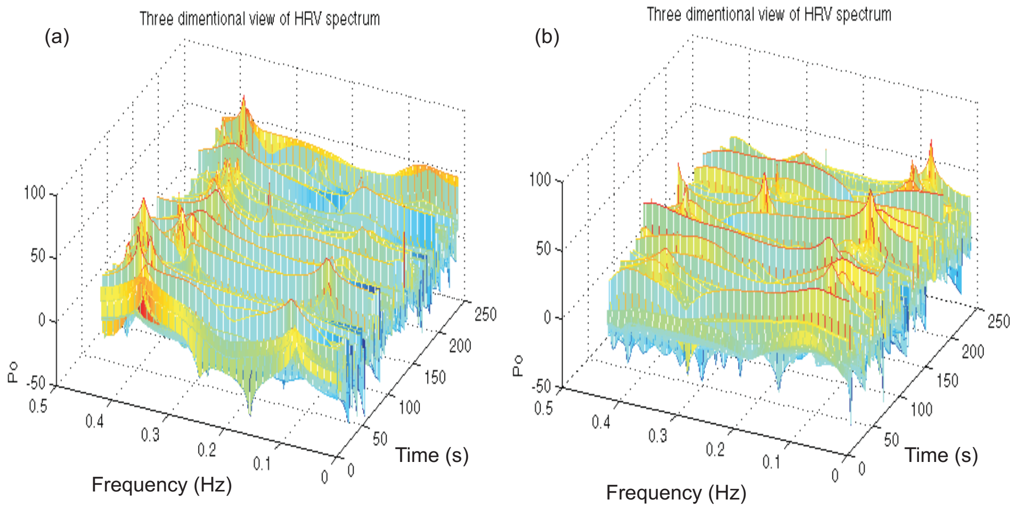

Figure 10. Three-dimensional view of the spectrum in control **(a)** and MI patient **(b)**.

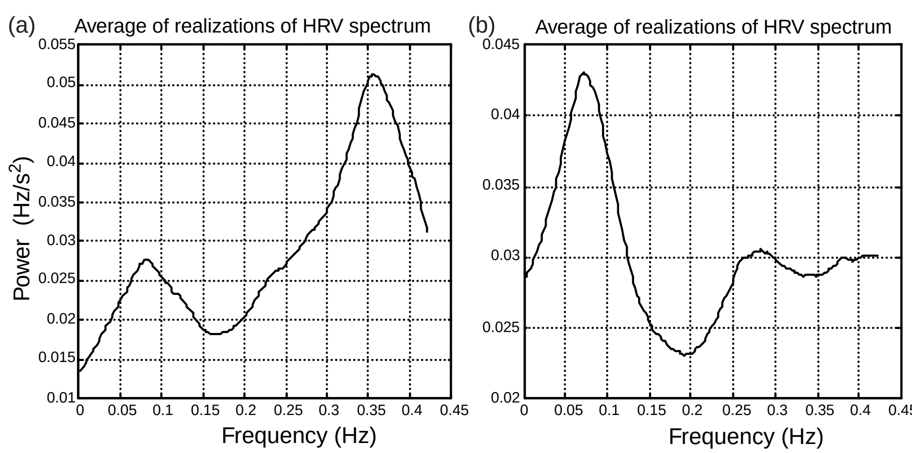

Figure 11. Average realisation of the spectrum in control **(a)** and MI patient **(b)**.

Table 1. Statistical results.

Subject	PRLH	PPRLH	TP	%PLF	%PHF
Control ($N = 25$)	$0{\cdot}859 \pm 0{\cdot}162$	$0{\cdot}859 \pm 0{\cdot}287$	$0{\cdot}073 \pm 0{\cdot}006$	$46{\cdot}06 \pm 5{\cdot}67$	$53{\cdot}94 \pm 5{\cdot}67$
Acute anterior MI patient ($N = 16$)	$1{\cdot}536 \pm 0{\cdot}388$	$1{\cdot}715 \pm 0{\cdot}541$	$0{\cdot}072 \pm 0{\cdot}005$	$59{\cdot}69 \pm 6{\cdot}12$	$40{\cdot}31 \pm 6{\cdot}12$
Acute inferior MI patient ($N = 9$)	$0{\cdot}737 \pm 0{\cdot}156$	$0{\cdot}78 \pm 0{\cdot}168$	$0{\cdot}069 \pm 0{\cdot}005$	$41{\cdot}98 \pm 5{\cdot}44$	$58{\cdot}02 \pm 5{\cdot}44$
P value	$<0{\cdot}005$	$<0{\cdot}005$	$0{\cdot}62$	$<0{\cdot}005$	$<0{\cdot}005$

The number of samples in a class is denoted by N. Parameter values in the table indicate the mean $\pm$ standard deviation and are calculated at 95% confidence level. Student-t test P values are found to be less than 0·005.

4. Conclusion

ARMA-based power spectral analysis of a heart-rate time series signal has been done. It can be concluded that parasympathetic activity is more prominent in controls and also that during acute myocardial infarction, the anterior wall MI is found to stimulate sympathetic activity, while the inferior wall MI is shown to stimulate marked parasympathetic activity. It is evident from the above observations that infarction can be detected using power spectral analysis of the HRT series. Thus, the results obtained from the above mentioned ARMA-based analysis of heart-rate time series signal are capable of complementing clinical examination, and thus leading to better diagnosis.

References

Baselli G, Cerutti S, Civardi S, Lombardi F, Malliani A, Merri M, Pagani M, Rizzo G 1987 Heart-rate variability signal processing: quantitative approach as an aid to diagnosis in cardiovascular pathologies. *Int. J. Biomed. Comput.* 51–70

Kay S M 1988 *Modern spectral estimation: Theory and application* (Englewood Cliffs, NJ: Prentice Hall) pp 17–33

Marple S L *Digital analysis with applications* (Englewood Cliffs, NJ: Prentice Hall)

Naidu V P S, Bindu E, Mahalakshmi P, Reddy M R S 1999 Spectral analy of heart-rate variability in myocardial infected patients. *Int. conf. on Medical Diagnostic Techniques and Procedures*, IIT Madras, Chennai, pp 76–81

Naidu V P S, Bindu E, Reddy M R S 2000 A high precision R-point detection algorithm. *Trends Biomater. Artif. Organs* vol. 14: 5–8

Natalucci S, Ruggeri P, Picchio V, C E Cogo, Burattini R 1999a Parametric analysis of heart-rate variability in anaesthetic SHR and WHY rats. *Comput. Cardiol.* 591–594

Natalucci S, Ruggeri P, Picchio V, Cogo C E, Burattni R 1999b Parametric analysis of heart-rate variability in anaesthetic SHR and WKY rats. *Comput. Cardiol.* : 591–594

Pagani M, *et al* 1976 Power spectral analysis of heart-rate and arterial pressure variabilities as a marker of sympatho-vagal interaction in man and conscious dog. *Circ. Res.* 49: 178–193

Pinna G, Orsi G, Corsio G 1992 Effect of record length on power spectral estimation of heart-rate variability signal. *Comput. cardiol.* 261–264